Cathodoluminescence of GaInN quantum wells grown on nonpolar *a* plane GaN: Intense emission from pit facets

K. J. Fujan,[1,a)] M. Feneberg,[1] B. Neuschl,[1] T. Meisch,[1] I. Tischer,[1] K. Thonke,[1] S. Schwaiger,[2] I. Izadi,[2] F. Scholz,[2] L. Lechner,[3] J. Biskupek,[3] and U. Kaiser[3]
[1]*Institut für Quantenmaterie/Gruppe Halbleiterphysik, Universität Ulm, 89069 Ulm, Germany*
[2]*Institut für Optoelektronik, Universität Ulm, 89069 Ulm, Germany*
[3]*Materialwissenschaftliche Elekronenmikroskopie, Universität Ulm, 89069 Ulm, Germany*

(Received 18 May 2010; accepted 18 August 2010; published online 9 September 2010)

$Ga_xIn_{1-x}N$ quantum wells grown by metal organic vapor phase epitaxy on *a* plane GaN grown on *r* plane sapphire substrate typically show relatively large surface pits. We show by correlation of low temperature photoluminescence, cathodoluminescence, scanning and transmission electron microscopy that the different semipolar side facets of these pits dominate the overall luminescence signal of such layers. © *2010 American Institute of Physics*. [doi:10.1063/1.3487935]

Non- and semipolar nitride semiconductor light emitting devices are of great interest due to their potentially high quantum efficiency. The reduced or vanishing polarization fields pave the way to a higher overlap of electron and hole wave functions leading to higher radiative transition matrix elements for such devices. Therefore, it is desirable to investigate non- and semipolar quantum well (QW) structures in more detail to gain insight into fundamental physical properties of related devices.

Here we present a comprehensive study on nonpolar *a* plane $Ga_xIn_{1-x}N$ grown by metal organic vapor phase epitaxy (MOVPE). Although the major part of the sample is smooth, it shows a surface morphology with stripelike features parallel to the *c* direction and, for our analysis more essential, surface pits. While there exist few samples without any pits, they are typical for *a* plane GaN and are known to consist of different semipolar facets. They remain visible even after $Ga_xIn_{1-x}N$ growth on an *a* plane GaN template. A representative example for such pits is shown in Fig. 1(b). Three different semipolar facets of this pit are marked according to Sun *et al.*[1] Although such pits are reported frequently in literature,[2–4] no systematic investigation regarding their luminescence properties is available up to now.

Two *a* plane samples are investigated in more detail [Fig. 1(a)]. Sample A was grown by MOVPE on *r* plane Al_2O_3 at a temperature of 1120 °C and a pressure of 150 hPa.[5] A first GaN layer of 1 μm thickness comprises an *in situ* SiN interlayer after 300 nm for defect reduction.[6] On top of a further SiN interlayer a second GaN layer with 2.3 μm thickness was grown.[7] For sample B, a multi quantum well (MQW) structure was grown on top of such a template, consisting of five QWs with nominally 10% indium. The QWs (barriers) were grown at 820 °C (885 °C) and 200 hPa. The structure was finally capped by a GaN layer of 20 nm thickness. Both samples show the typical surface morphology with pits and are analyzed by scanning electron microscopy (SEM), by high angle annular dark-field (HAADF) scanning transmission electron microscopy (STEM), as well as by low temperature cathodoluminescence (CL) and photoluminescence (PL). The major part of the sample surfaces is smooth. By atomic force microscopy the average pit density was found to be $\approx 9\times10^5$ cm^{-2}. This value slightly increases toward the edge of the wafer. Most of the pits are $\approx 2\mu$m in diameter with a few extending up to 10 μm.

Temperature dependent PL measurements on both samples show characteristic differences (Figs. 2 and 3). Apparently, the broad structureless bands around 2.9 eV, as well as the bands (2) and (3) in Fig. 3 at 3.35 eV and 3.38 eV (at 10 K) are only prominent in sample B and are therefore related to the $Ga_xIn_{1-x}N$ QWs, whereas the peaks marked by stars (*) are present in both samples, no matter if QWs are grown or not. Therefore we assign these latter peaks to common structural defects present in *a* plane GaN, especially the basal plane stacking fault of type I_1.[8,9] For the band at 3.32 eV several origins are discussed in the literature.[9–12]

For sample B with $Ga_xIn_{1-x}N$ MQW, we find in the region around 3.35 eV the peaks labeled (2) and (3) (Fig. 3). According to their very similar spatial distribution found in monochromatic CL images [see below Figs. 5(c) and 5(d)], they must be introduced by the presence of the MQW on the *a* plane, and seemingly are closely related. Upon temperature increase, they change their relative intensity (see Fig. 3). Most probably, slightly different thickness or In content of the stacked QWs leads to the occurrence of two peaks instead of one.

The presence of different MQW related emission bands and surface pits raises the natural question concerning the spatial origin of the different transitions. Therefore, we investigated these samples in more detail by spatially highly resolved SEM CL.

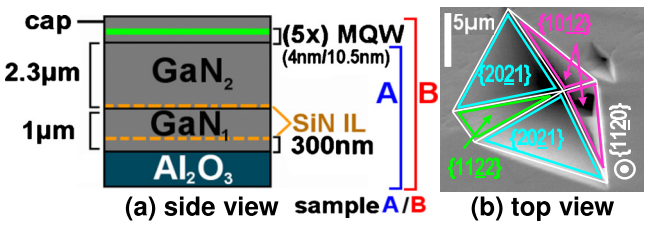

FIG. 1. (Color online) (a) Scheme of the sample structure: Sample A consists only of the layers up to the 2.3 μm thick GaN buffer, while sample B has additionally a fivefold QW and a capping layer on top. SiN IL marks SiN_X interlayers inserted for defect reduction. (b) Scanning electron micrograph of a typical surface pit with marked facet types.

a)Electronic mail: kim.fujan@uni-ulm.de.

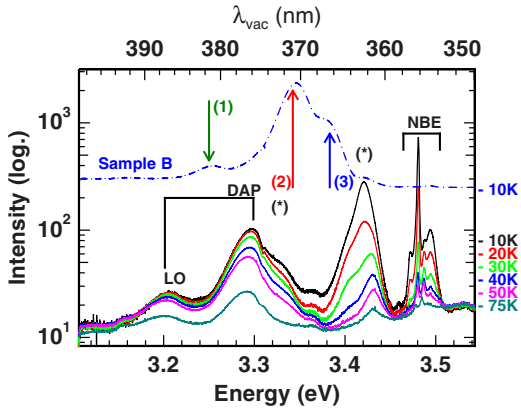

FIG. 2. (Color online) Temperature dependent PL spectra of sample A (without MQW) showing the near band gap emission bands. For comparison a spectrum of sample B (with MQW, 10 K) is plotted as well (vertically shifted for clarity, dotted-dashed blue line).

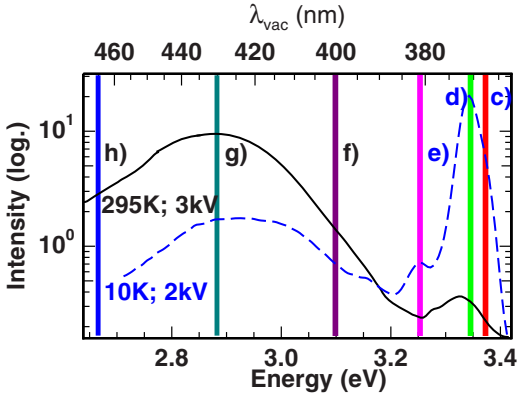

FIG. 4. (Color online) Logarithmic CL spectra of sample B at the position shown in Fig. 5(a). Spectra at 10 K (blue, dashed) and 295 K (black) were recorded with an excitation voltage of 2 kV and 3 kV, respectively. Vertical lines correspond to the monochromatic CL images visible in Figs. 5(c)–5(h). Corresponding features are denoted with the same letter.

Spatially integrated CL spectra of sample B are shown in Fig. 4. The corresponding excitation region is visible in Fig. 5(a) and consists of a rectangle of approximately 15 $\times 15$ μm. For increasing temperature, the low energy MQW related band increases in relative intensity, whereas the higher energy bands become weaker. The energy ranges of interest, used for the corresponding monochromatic CL micrographs shown in Figs. 5(c)–5(h), are marked by vertical colored bars in Fig. 4.

From Fig. 5 it is evident that different transition energies are emitted selectively from different non- and semipolar surfaces. While the three higher energy contributions [shown in Figs. 5(c)–5(e)], recorded at 10 K, originate from the nonpolar *a* plane surface, the low energy bands [Figs. 5(f)–5(h)], recorded at 295 K, originate from different facets within the pits. By combination of PL spectra (Fig. 3) and CL images (Fig. 5) we can assign the occurring peaks to their respective origin. The three emission bands at 3.37, 3.34, and 3.25 eV are from the QW grown on the *a* plane since they are not observed without QW (Fig. 2). The band at 3.25 eV [peak (1) in Figs. 2 and 3] shown in the CL image in Fig. 5(e) stems from small sharply separated linelike features scattered over the *a* plane. Because these lines are oriented perpendicular to the *c* direction, we tentatively assign them to the basal plane stacking fault related radiation from within the $Ga_xIn_{1-x}N$ QW layer due to their absence in sample A. The spatial intensity distribution of this band [Fig. 5(e)] is clearly anticor-

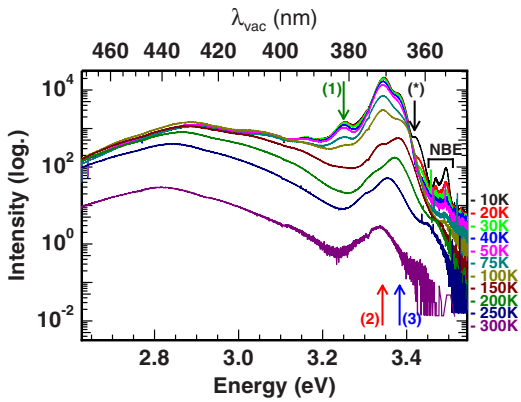

FIG. 3. (Color online) Temperature dependent PL measurements of sample B (with MQW). Contributions discussed in the text are marked with arrows.

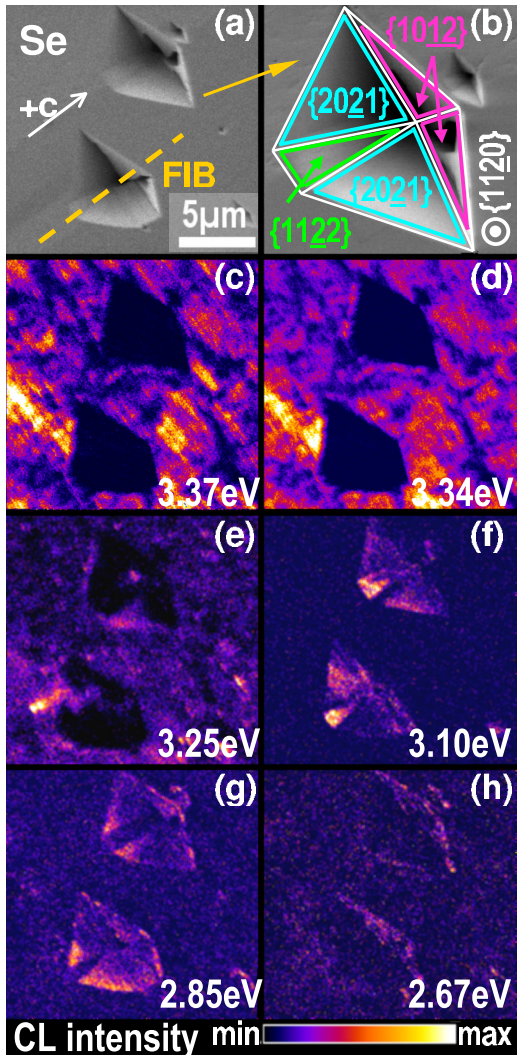

FIG. 5. (Color online) SEM secondary electron (Se) picture of the investigated region of the sample with QWs (a), and monochromatic CL images of exactly the same sample region recorded at 3.37 eV (c), 3.34 eV (d), and 3.25 eV (e) at 10 K, as well as 3.10 eV (f), 2.88 eV (g), and 2.67 eV (h) at room temperature. Picture (b) shows a more detailed view on such a pit. The facet types are marked and assigned according to Sun *et al.*

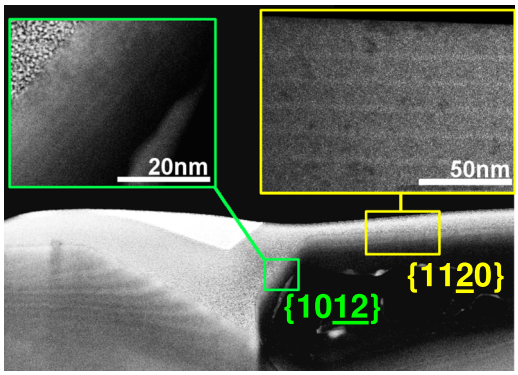

FIG. 6. (Color online) HAADF-STEM image of a representative pit of sample B after focused ion beam preparation. The fivefold $Ga_xIn_{1-x}N/GaN$ QWs are clearly visible by their atomic mass contrast in the enlarged cutouts of the *r* plane on the left and the *a* plane on the right hand side.

related with the emission at 3.37 eV [Fig. 5(c)] and also different from the emission at 3.34 eV [Fig. 5(d)]. Thus, the 3.25 eV line cannot be the LO replica of peak (2) at 3.34 eV.

The mappings of the emission bands attributed to the $Ga_xIn_{1-x}N$ MQW grown on the different semipolar facets of the pits are shown in Figs. 5(f)–5(h). The 3.10 eV band originates mainly from the {11$\bar{2}$2} facet, the 2.85 eV band from the {20$\bar{2}$1} facet, and the band centered around 2.67 eV stems from the *r* plane or {10$\bar{1}\bar{2}$} facet only. From CL alone we cannot separate changes in QW thickness and changes in indium incorporation, which additionally lead to different polarization fields in the QWs on the different facets. Therefore, we used focused ion beam technique to prepare a representative pit for STEM investigation [cut direction marked by the yellow dashed line in Fig. 5(a)]. The STEM results are shown in Fig. 6. From the STEM data we get the QW width in the {11$\bar{2}$0} and {10$\bar{1}\bar{2}$} QWs, which are about 4 nm and 2.5 nm, respectively. For their counterparts on the {20$\bar{2}$1} and {11$\bar{2}$2} facets no STEM images are available, but we assume them to have similar QW thicknesses between 2.5 and 4 nm. The observed thicknesses and In contents resulting from CL emission are summarized in Table I. Taking polarization fields into account, this leads to indium concentrations between 3% and 24%. Therefore, the differences in emission wavelengths are mainly dependent on different In incorporation rather than different QW thicknesses. Thus, we conclude that the incorporation efficiency of In is very different on the investigated facet types leading to the order {10$\bar{1}\bar{2}$} > {20$\bar{2}$1} > {11$\bar{2}$2} > {11$\bar{2}$0} (from higher to lower indium incorporation efficiency).

TABLE I. Summary of STEM and CL results in terms of indium (In) content for different facets with variable thickness of the InGaN MQW including the different polarization fields on the different facets.

Facet type	{10$\bar{1}\bar{2}$} *r* plane	{20$\bar{2}$1}	{11$\bar{2}$2}	{11$\bar{2}$0} *a* plane
CL peak energy (eV)	2.67	2.85	3.10	3.34
STEM: w_{QW} (nm)	≈2.5	N.A.	N.A.	≈4
Calculated In content for				
w_{QW}=4 nm	···	0.10	0.057	0.03
w_{QW}=2.5 nm	0.24	0.13	0.074	···

In summary, we investigated by luminescence techniques including monochromatic CL images the origin of several $Ga_xIn_{1-x}N$ QW related transmission bands in *a* plane $Ga_xIn_{1-x}N/GaN$ MQWs. We find that the indium incorporation is much higher on the semipolar facets within the pits than on the surface. The QWs in the pits seemingly capture excited electron-hole pairs very efficiently and dominate with their emission the entire PL or CL spectrum at room temperature. Considering this, caution is necessary in the interpretation of PL spectra from $Ga_xIn_{1-x}N$ QWs grown on semipolar surfaces when pits exist, as typically is found for such layers.

[1]Q. Sun, C. D. Yerino, T. S. Ko, Y. S. Cho, I. Lee, J. Han, and M. E. Coltrin, J. Appl. Phys. **104**, 093523 (2008).
[2]J. N. Dai, Z. H. Wu, C. H. Yu, Q. Zhang, Y. Q. Sun, Y. K. Xiong, X. H. Han, L. Z. Tong, Q. H. He, F. A. Ponce, and C. Q. Chen, J. Electron. Mater. **38**, 1938 (2009).
[3]M. D. Craven, S. H. Lim, F. Wu, J. S. Speck, and S. P. DenBaars, Appl. Phys. Lett. **81**, 469 (2002).
[4]T. S. Ko, T. C. Wang, R. C. Gao, H. G. Chen, G. S. Huang, T. C. Lu, H. C. Kuo, and S. C. Wang, J. Cryst. Growth **300**, 308 (2007).
[5]S. Schwaiger, F. Lipski, T. Wunderer, and F. Scholz, Phys. Status Solidi C **7–8**, 2069 (2010).
[6]A. Chakraborty, K. C. Kim, F. Wu, J. S. Speck, S. P. DenBaars, and U. K. Mishra, Appl. Phys. Lett. **89**, 041903 (2006).
[7]J. L. Hollander, M. J. Kappers, C. McAleese, and C. J. Humphreys, Appl. Phys. Lett. **92**, 101104 (2008).
[8]C. Stampfl and C. G. Van de Walle, Phys. Rev. B **57**, 15251 (1998).
[9]R. Liu, A. Bell, F. A. Ponce, C. Q. Chen, J. W. Yang, and M. A. Khan, Appl. Phys. Lett. **86**, 021908 (2005).
[10]Y. J. Sun, O. Brandt, U. Jahn, T. Y. Liu, A. Trampert, S. Cronenberg, S. Dhar, and K. H. Ploog, J. Appl. Phys. **92**, 5714 (2002).
[11]P. P. Paskov, R. Schifano, B. Monemar, T. Paskova, S. Figge, and D. Hommel, J. Appl. Phys. **98**, 093519 (2005).
[12]I. Tischer, M. Feneberg, M. Schirra, H. Yacoub, K. Thonke, R. Sauer, T. Wunderer, F. Scholz, L. Dieterle, E. Müller, and D. Gerthsen, "I_2 basal plane stacking fault in GaN: origin of the 3.32 eV luminescence band," Phys. Rev. B (submitted).